



**HAL**  
open science

## Towards an experimental approach for measuring the removal of urban air pollutants by green roofs

Yara Arbid, Claire Richard, Mohamad Sleiman

### ► To cite this version:

Yara Arbid, Claire Richard, Mohamad Sleiman. Towards an experimental approach for measuring the removal of urban air pollutants by green roofs. *Building and Environment*, 2021, 205, pp.108286. 10.1016/j.buildenv.2021.108286 . hal-03329684

**HAL Id: hal-03329684**

**<https://hal.science/hal-03329684>**

Submitted on 8 Sep 2021

**HAL** is a multi-disciplinary open access archive for the deposit and dissemination of scientific research documents, whether they are published or not. The documents may come from teaching and research institutions in France or abroad, or from public or private research centers.

L'archive ouverte pluridisciplinaire **HAL**, est destinée au dépôt et à la diffusion de documents scientifiques de niveau recherche, publiés ou non, émanant des établissements d'enseignement et de recherche français ou étrangers, des laboratoires publics ou privés.

1                   Towards an experimental approach for  
2 measuring the removal of urban air pollutants by  
3                   green roofs

4                   Yara Arbid, Claire Richard, Mohamad Sleiman\*

5 University Clermont Auvergne, CNRS, Clermont Auvergne INP, Institut de Chimie de Clermont-Ferrand  
6 F-63000 Clermont-Ferrand, France

7 [Yara.arbid@etu.uca.fr](mailto:Yara.arbid@etu.uca.fr)

8 [Claire.richard@uca.fr](mailto:Claire.richard@uca.fr)

9 [Mohamad.sleiman@sigma-clermont.fr](mailto:Mohamad.sleiman@sigma-clermont.fr)

10 \*Corresponding author: Mohamad Sleiman – University Clermont Auvergne, CNRS, Clermont Auvergne  
11 INP, Institut de Chimie de Clermont-Ferrand F63000 Clermont-Ferrand, France; orcid.org/0000-0002-  
12 2273-1053; Email: Mohamad.sleiman@sigma-clermont.fr

## 13 **ABSTRACT**

14           Green roofs are a promising approach to mitigate air pollution in urban environments, but limited  
15 experimental data is yet available. In this study, we developed a laboratory-scale setup to measure the  
16 removal nitrogen dioxide (NO<sub>2</sub>) and ozone (O<sub>3</sub>) using a variety of common green roof species.  
17 Experiments were conducted on detached leaves and whole plants using two chambers (0.6 L and 12 L),  
18 visible lighting, NO<sub>x</sub>/O<sub>3</sub> sources and online analyzers. Three species were the best performant (Thymus  
19 vulgaris, Sedum sexangulare and Heuchera Americana L.) with deposition velocities ( $v_d$ ) ranging from  
20 1.6 to 4.82 m/h for NO<sub>2</sub>, and 1.7 to 5.56 m/h for O<sub>3</sub>. In both cases, thyme was the most effective plant  
21 likely due to its higher stomatal area and the reactivity of its volatile metabolites with O<sub>3</sub> leading to  
22 several oxidized by-products. Furthermore, NO<sub>2</sub> uptake was found to be enhanced by surface water  
23 released by leaf transpiration leading to the production of nitrous acid (HONO). Similar values of ( $v_d$ )  
24 were observed (3.84 – 4.65 m/h) when whole thyme plant was used. The soil was also found to be  
25 competitive in removing O<sub>3</sub> but less performant in capturing NO<sub>2</sub>. Using a dry deposition model, we  
26 estimated that the three plant species can uptake up to 9 kg/ha/year of NO<sub>2</sub> and 13.6 kg/ha/year, which fall  
27 in agreement with previously reported modeling data. Our experimental approach can be a rapid tool for  
28 screening the depollution performances of green roof species enabling an effective prioritization for  
29 deployment in urban environments.

30 Keywords: Green roofs, air pollution, NO<sub>x</sub>, O<sub>3</sub>.

## 31 **1. INTRODUCTION**

32           Outdoor air pollution causes up to 10 million deaths annually, and around 90 % of the world  
33 population live in urban environments where air pollution exceeds the World Health Organization (WHO)  
34 limits [1]. Air pollution mitigation strategies such as source reduction (electrical vehicles [2], fuel and  
35 traffic regulations [3], renewable energy resources [4], etc.), and depollution technologies have been  
36 increasingly adopted in the recent years. Among depollution methods, the use of highly reflective

37 photocatalytic roofs and walls [5] have been shown to be effective in reducing the urban heat island effect,  
38 and in the removal of Volatile Organic Compounds (VOCs) and Nitrogen Oxides (NO<sub>x</sub>) [6,7]. However,  
39 photocatalytic oxidation process can lead to the formation of toxic intermediates and the VOC removal  
40 performance can decrease over time [8]. Another promising alternative is the use of natural walls and  
41 roofs such as vertical greening systems or green roofs which can be a replacement to conventional roofs  
42 especially in crowded urbanized areas [9]. Green roofs have been receiving attention recently as effective  
43 nature-based solution to eco-environmental problems arising from climate change and rapid urbanization  
44 [10]. They can retain storm water via absorption into the substrate [11,12], reduce the building energy  
45 demand by improving the thermal insulation [13], lower noise pollution [14], in addition to improving the  
46 roof aesthetic values.

47         Plants used in such green roofs are able to mitigate air pollution [15] by absorbing the pollutants  
48 through their stomata via dry deposition on the surfaces of leaves [16]. Urban trees and shrubs are known  
49 to remove efficiently air pollutants [17]. Reactive pollutants (O<sub>3</sub>, NO<sub>x</sub>, SO<sub>2</sub>) can be removed by  
50 absorption via stomata or by surface uptake via potential chemical reactions with volatile metabolites such  
51 as terpenes. On the other hand, the formed particulate matter (PM) can be removed via deposition on the  
52 leaf surface. The performance depends on various factors such as the proximity of the vegetation to the  
53 road and its height [18]. Although trees are a very effective strategy in controlling pollution, planting trees  
54 in crowded cities with high percentages of impervious areas is challenging. Thus, in metropolitan cities,  
55 green roofs can be an alternative solution to make use of rooftops [19]. Several modelling studies showed  
56 that green roofs can be efficient in removing various prevalent air pollutants. According to Yang et al.,  
57 22.8 kg/ha/year of NO<sub>2</sub> and around 44 kg/ha/year of O<sub>3</sub> can be eliminated using green roofs [16]. Grass  
58 was found effective in removing O<sub>3</sub> (5.2 kg/ha/year) whereas, shrubs have the potential to eliminate 18  
59 kg/ha/year of PM<sub>10</sub> [20]. Speak et.al [21] showed that sedum, a widely used plant species on extensive  
60 green roofs, could remove 4.2 kg/ha/year of PM<sub>10</sub>. However, most aforementioned studies were based

61 solely on modelling using estimated deposition velocities ( $v_d$ ) which can vary significantly depending on  
62 the plant species, seasonality, climate, etc.

63 To the best of our knowledge, the air depollution performance of green roofs species has been  
64 very little investigated, and only limited recent data exist on their efficiency in the laboratory and in the  
65 field [22,23]. Performance-based laboratory screening measurements –in combination with field  
66 campaigns- are thus needed to improve the precision of models and to provide a valuable tool for  
67 implementing the best performant species as a function of target pollutants. In this study, we developed an  
68 experimental setup to measure the NO<sub>x</sub>/O<sub>3</sub> uptakes of 13 plants commonly used on green roofs. After  
69 initial screening, 3 species were selected (*Sedum sexangulare*, *Thymus vulgaris*, and *Heuchera micrantha*  
70 *palace purple*). The removal rates of these plants were investigated using detached leaves as well as full  
71 size plants. This work aimed to guide in the choice of plants to be used on green roofs according to the  
72 need of targeting a specific pollutant in an urbanized area, and to get insight into the mechanisms taking  
73 place.

## 74 **2. MATERIALS AND METHODS**

### 75 **2.1. Chemicals and materials**

76 Imidacloprid (IMD) was purchased from Sigma Aldrich, Switzerland (Pestanal™, analytical standard,  
77 ≥98.0% purity HPLC area %). Sodium carbonate anhydrous was purchased from Fluka, Germany  
78 (≥99.5% purity ACS). Both were used without further purification. Water was produced using a reverse  
79 osmosis RIOS 5 and Synergy (Millipore) device (resistivity 18 MΩ cm, DOC<0.1 mg L<sup>-1</sup>). Acetonitrile  
80 (ACN) was purchased from Carlo Erba Reagents (HPLC Plus Gradient grade-ACS-Reag.

81 Process of plant selection: Green roofs vary from intensive to extensive roofs differing in the maintenance  
82 needs, substrate depth, plants implemented, etc. Contrarily to intensive ones where shrubs or even trees  
83 may be implemented, extensive green roofs use shallow root plants and thus are more commonly used due  
84 to their low maintenance needs and lightweight. Hence, in this study, we solely focused on extensive  
85 green roof species which are drought tolerant such as grasses, perennials, and succulents. Based on

86 literature review, and after careful consideration of weather conditions in central France, 13 species were  
87 selected for screening: *Achillée millefeuille paprika*, *Achillea umbellata à feuillage gris*, *Alchemille jaune*,  
88 *Aster des alpes rose*, *Heuchera americana L.*, *Joubarbe calcareum*, *Joubarbe rubin*, *Thymus nummularius*,  
89 *Sedum floriferum jaune*, *Sedum reflexum jaune*, *Sedum sexangulare*, *Sedum spurium*, and *Thymus*  
90 *vulgaris*. After pre-screening, three species were chosen to further investigate their performance for the  
91 removal of O<sub>3</sub> and NO<sub>2</sub>: *Sedum sexangulare*, *Thymus vulgaris*, *Heuchera americana L.*

92 Conditions for plant storage and care: Plants were stored in an indoor greenhouse exposed to outdoor  
93 sunlight through a large window and were watered every two days. Temperature was between 20-25 ° C  
94 in the greenhouse during storage and around 23°±2 C when used in the laboratory. Relative humidity (RH)  
95 was ranged between 30-55%.

96 *Sedum sexangulare*, *Thymus vulgaris*, and *Heuchera micrantha palace purple* were purchased from a  
97 plant nursery (Botanic®, Beaumont, France) and watered every two days. These species are used on green  
98 roofs and different studies report their performance towards different air pollutants [24–26].

99 *Sedum sexangulare* (sedum): Sedum species are considered as appropriate plants to be applied on  
100 extensive green roofs. They are drought tolerant and can survive in harsh climate conditions. In the  
101 literature, *Sedum sexangulare* showed a good performance under severe climate conditions and that it is  
102 suitable to be implemented in a Mediterranean climate [24].

103 *Thymus vulgaris* (thyme): Thyme is an odorous perennial plant used on green roofs. It emits different  
104 VOCs (**Fig.SI-1.**) which can react with air pollutants [25].

105 *Heuchera Americana L.* (heuchera): Heuchera species are used in vertical greenery systems and green  
106 roofs because their colorful glossy leaves give them important aesthetics values. Heuchera retains  
107 different elements and particulate matter (PM) due to its hairy undersides [26].

108 Plants were stored in an indoor greenhouse with direct solar light. They were either used directly as a full-  
109 size plant (pot size: 9-15 cm) or their leaves cut using scissors into pieces of 0.9-1.2 g prior to the  
110 experiment.

111 To avoid changes induced by diurnal cycles, all experiments using plants were performed during the day  
112 from 10 am to 3 pm. The planting soil was a universal soil with a water retention capacity of 75%,  
113 pH=6.5, and N, P, K values of 5.5, 2.5, and 1.5 for 2 kg/m<sup>3</sup> respectively.



114  
115 **Fig.1.** Pictures of the 3 studied plants: *Sedum sexangulare*, *Thymus vulgaris*, and *Heuchera Americana L.*  
116 (left to right).

## 117 2.2. Experimental setup

118 A new experimental setup was designed to measure the uptakes of leaves and the full-size plant  
119 under irradiation with NO<sub>x</sub> and O<sub>3</sub> configurations.

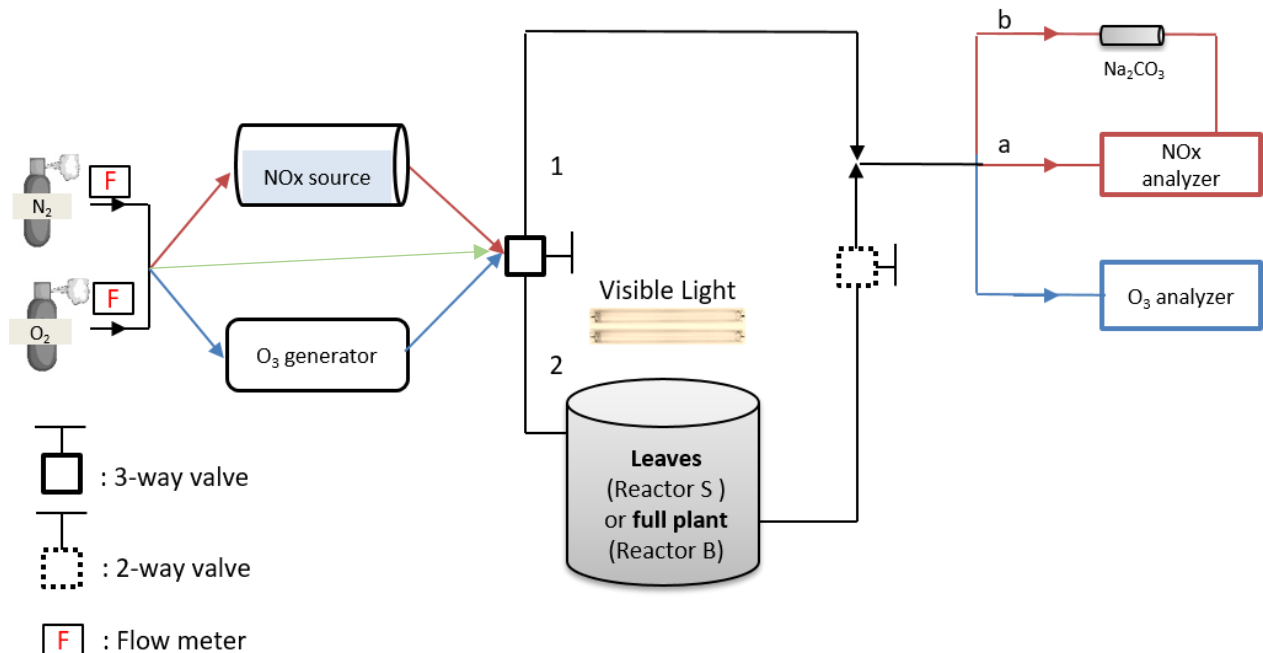


**Fig.2.** Experimental setup used for measuring the uptake of NO<sub>2</sub> (red) and O<sub>3</sub> (blue).

120 NO<sub>x</sub>/O<sub>3</sub> setup The setup includes:

- 121 1. Two flow meters (Brooks 4800 series/ 50-500 ml/min) to regulate the flow of O<sub>2</sub> and N<sub>2</sub>  
 122 simultaneously mimicking the ratio of these gases in ambient air.  
 123 2. An NO<sub>x</sub> source via a 200 ml solution of IMD (10<sup>-5</sup> M) producing 40-50 ppbv of NO<sub>2</sub> and 0.1-0.5  
 124 ppbv of NO contained in a cylindrical Pyrex glass flow-reactor (0.65 L, length 27 cm and internal  
 125 diameter 5.7 cm). This was based on our previous study showing that irradiating a solution of  
 126 IMD with a polychromatic light ( $\lambda_{\max}$ = 365 nm) leads to the production of NO<sub>x</sub> (NO + NO<sub>2</sub>) with  
 127 NO<sub>2</sub> being the major product [27].

128 A UVP ozone generator equipped with a UV pen-ray lamp that uses the photochemical reaction of  
 129 O<sub>2</sub> under UVC (185 nm) to produce the continuous flow of O<sub>3</sub>.

- 130 3. Two air-tight stainless-steel reactors (see **Fig.SI-2.**) that are cylindrical with a Pyrex glass top  
 131 window for irradiation. A small one (Reactor S- 0.6 L) for leaves and a big reactor (Reactor B- 12  
 132 L) for the full-size plant.



- 133 4. 2x55W Starlite tubes ( $\lambda= 400-800$  nm) that were placed at a distance of  $\approx 30$  cm above the reactors  
 134 for irradiation. Absolute Irradiance at this distance was  $6-7 \mu\text{W}/\text{cm}^2/\text{nm}$  @ 610 nm. This lamp is  
 135 commonly used for growing plants indoors where it covers the light range needed for  
 136 photosynthesis (see spectrum **Fig.SI-3**).
- 137 5. A NO<sub>x</sub> Thermo scientific 42i model-NO NO<sub>2</sub> NO<sub>x</sub> analyzer (chemiluminescence analyzer). To  
 138 measure the nitrous acid (HONO) and estimate its contribution to the NO<sub>2</sub> measured levels, a  
 139 Na<sub>2</sub>CO<sub>3</sub>-impregnated quartz filter was installed upstream of the NO<sub>x</sub> monitor, to trap HONO. Its  
 140 concentration was then calculated by measuring the difference between measured NO<sub>2</sub> values with  
 141 and without the HONO scrubber.
- 142 An O342e ozone analyzer O<sub>3</sub> (Environnement S.A). Both analyzers were online real-time  
 143 analyzers with a 10 s temporal resolution.

144 The tubes used were PTFE (Teflon) to minimize secondary reactions, the fitting and valves were stainless  
 145 steel from Swagelok (Lyon-France), and the temperature was regulated to 23 °C by an air conditioner.

### 146 2.3. Calculation of deposition velocities and plant uptake coefficients

147 For the plants tested in this study, transient deposition velocities ( $v_d$ ) for NO<sub>2</sub> and O<sub>3</sub> were calculated,  
 148 similar to Poppendieck et al. [28] and Abbass et al.[29], based on a mass balance that is shown in equation  
 149 (1):

$$150 \quad \frac{dC_{out}}{dt} = \lambda(C_{in} - C_{out}) - v_{d(p)}C_{out} \frac{A_{(p)}}{V} - v_{d(c)}C_{out} \frac{A_{(c)}}{V} \quad (1)$$

151 Where  $\frac{dC_{out}}{dt}$  represents the change in the outlet O<sub>3</sub> or NO<sub>2</sub> concentration (ppb h<sup>-1</sup>), C<sub>in</sub> and C<sub>out</sub>  
 152 are the outlet concentration of NO<sub>2</sub> or O<sub>3</sub>, in the inlet and the outlet of the exposure chamber  
 153 (ppbv), respectively,  $\lambda$  is the air exchange rate for the chamber (h<sup>-1</sup>),  $v_{d(p)}$  and  $v_{d(c)}$  are the  
 154 deposition velocities for a plant and chamber (m/h), respectively,  $A_{(p)}$  and  $A_{(c)}$  are the exposed

155 area of the plant and chamber walls ( $m^2$ ), respectively. Eq. (1) was solved for the transient deposition  
156 velocity shown in equation (2):

$$157 \quad v_{d(p)}^t = \frac{V}{A_{(p)}} \frac{1}{C_{out}^t} \left[ \lambda (C_{in}^t - C_{out}^t) - v_{d(c)} C_{out} \frac{A_{(c)}}{V} - \frac{C_{out}^t - C_{out}^{t+1}}{\Delta t} \right] \quad (2)$$

158 Where  $v_{d(p)}^t$  is the time varying deposition velocity for a plant, t and t indicate consecutive data  
159 points (h), V is the volume of the test chamber. The deposition velocity associated with chamber  
160 walls  $v_{d(c)}$  was observed to be negligible for all experiments. To facilitate comparison across  
161 plants, the near steady-state deposition velocity was calculated when the rate of change in exit  
162 concentration was less than 2 ppb over 15 min. The uptake coefficients  $U_p^t$  were then calculated  
163 by multiplying the deposition velocity  $v_{d(p)}^t$  by the inlet concentration of  $NO_2$  or  $O_3$  ( $C_{in}^t$ ) after  
164 its conversion from ppbv to  $\mu g/m^3$  (eq. 3).

$$165 \quad U_p^t = v_{d(p)}^t (C_{in}^t) \quad (3)$$

#### 166 2.4. Analytical methods

167 *VOC analysis.* The composition of VOC produced by the three plant species was determined using  
168 headspace gas chromatography coupled with mass spectrometry detection (HS-GC/MS; Shimadzu HS-20  
169 coupled with QP2010SE). 1 g of leaves from each species was transferred into a 20 mL headspace glass  
170 vial and incubated for 10 min at 80 °C. The analytical column (Mega 5-MS 30 m  $\times$  0.25 mm) was  
171 operated initially at 60°C for 1 min, followed by an 8°C  $min^{-1}$  ramp to reach 240°C and held for 4 min.  
172 The mass spectrometer source was heated to 200°C, and signals were detected between mass to charge  
173 ratios (m/z) of 50 and 350. Identification of the major constituents was carried out using the NIST 17  
174 database and when necessary, using authentic standards.

175 *ATD-GC-MS*. After the ozonation of thyme leaves, the reactor gas phase was sampled for 3 min at a  
176 sampling rate of 100 mL min<sup>-1</sup> into the Tenax sorbent tubes. After sampling, the tubes were thermally  
177 desorbed using TurboMatrix thermal desorption unit (ATD 150, Perkin Elmer) equipped with a cold trap  
178 (Carbotrap 300) and coupled to an Agilent 6890 gas chromatograph and an Agilent 5973 mass  
179 spectrometry detector. The separation of desorbed volatiles was carried out using a HP-5  $\mu$ s column (25 m  
180  $\times$  0.25 mm  $\times$  0.25  $\mu$ m) operated initially at 50 °C for 1 min, followed by a 10°C/min ramp to reach 230°C.  
181 Mass spectra were scanned between m/z 35 and m/z 350 with the source temperature set at 20°C.

182 *HPLC-DAD*. HPLC analyses were performed using a NEXERA XR HPLCDAD apparatus. Separation  
183 was conducted using a phenomenex reversed phase C18 column (100 mm  $\times$  2.1 mm, 2.6  $\mu$ m particle size)  
184 and a binary solvent system composed of 10% acetonitrile and 90% water at a flow of 0.2 mL/min.  
185 Analysis time was 10 minutes. HPLC analyses allowed the monitoring of thymol disappearance as well as  
186 its absorption spectrum.

187 *Scanning electron microscopy (SEM)*. The structure of thyme cuticular surfaces before and after ozonation  
188 were characterized using scanning electron microscope. Leaves were mounted on aluminum stubs using  
189 double-sided adhesive tape and sputter-coated with 10-15 nm gold-palladium (20 s, 25 mA, partial argon  
190 pressure 60 mTorr, Denton Desk V. The samples were investigated with a field-emission scanning  
191 electron microscope (SH 4000 M) using a 20 kV acceleration voltage and a 10 mm working distance.  
192 Pictures were taken from adaxial and abaxial leaf surfaces.

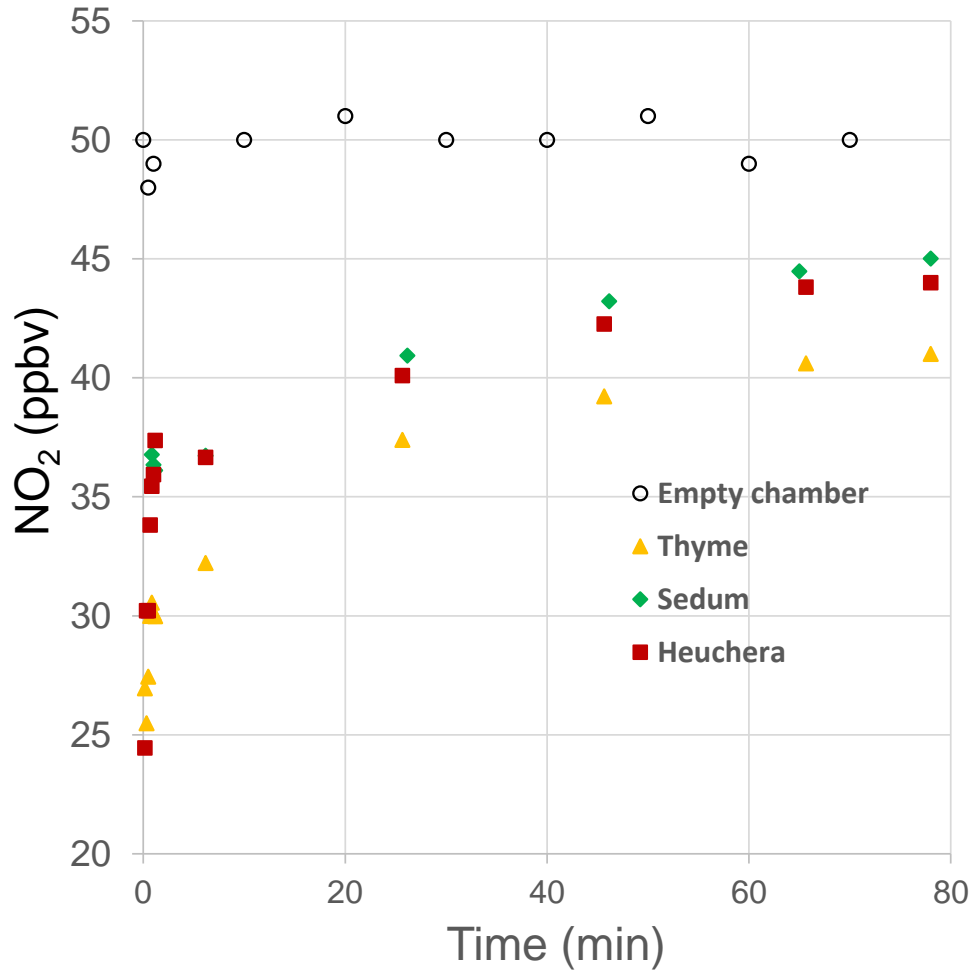
### 193 **3. RESULTS AND DISCUSSION**

#### 194 3.1. Depollution capacity of detached leaves

##### 195 3.1.1. NO<sub>2</sub> uptake

196 A maximum of 1 g of leaves was irradiated in the reactor for 1 hr while being ventilated with pure  
197 synthetic air at a flow rate of 0.8 L/min (green line in Fig. 2) under visible light allowing the plant to adapt  
198 to the conditions given before measuring the uptake. During this period, NO<sub>2</sub> generated by IMD was

199 directly monitored and its average concentration was found to be relatively stable around  $50 \pm 2$  ppbv.  
200 Following the 1 h pre-conditioning of the plant, NO<sub>2</sub> gas flow was introduced into the reactor containing  
201 the detached leaves and the NO<sub>2</sub> concentration was monitored initially every 10 seconds and then  
202 regularly until reaching a steady-state to calculate the NO<sub>2</sub> uptake. In control experiment, NO<sub>2</sub> flow was  
203 passed through empty chamber (no leaves) and its concentration showed negligible drop suggesting a  
204 negligible background removal of NO<sub>2</sub> due to chamber walls (See Fig. 3). In the presence of detached  
205 leaves of green roof species, the chamber exit concentration of NO<sub>2</sub> concentration increases quickly in the  
206 first minute as the chamber is filled with constant level NO<sub>2</sub> followed by a slower and progressive  
207 increases until approaching a steady-state after 1h of exposure. At the end of the experiment, thyme  
208 showed the highest NO<sub>2</sub> uptake with a reduction of about 9 ppbv in NO<sub>2</sub> concentration followed by sedum  
209 and heuchera with a reduction of about 5-6 ppbv. The near steady-state deposition velocities for the three  
210 plants were calculated by averaging the last 15 min of the exposure.



211 **Fig.3.** Empty chamber and outlet NO<sub>2</sub> concentration for sedum, thyme, and heuchera.

212 **Table 1** shows the near steady-state NO<sub>2</sub> deposition velocities and corresponding uptake coefficients  
 213 for the three plant species tested. While Heuchera seems to perform as good as sedum according to Fig. 3,  
 214 the exposed surface of its leaves was twice higher than that for Sedum and Thyme due to its large leaves.  
 215 Yang et al [16] estimated the removal capacity of 71 green roofs using a big leaf dry deposition model and  
 216 reported an average uptake coefficient of 260 μg/m<sup>2</sup>/h for NO<sub>2</sub> which is comparable to the values reported  
 217 in this study. In addition, the calculated  $v_{d(p)}^t$  (1.70 – 5.56) fall also within the range of  $v_d$  in their model  
 218 (0.36 – 21.6 m/h). Our values are also in agreement with those reported by Currie and Bass [20] who used  
 219 the UFORE model (urban forest effects model) and grass as a proxy unit for green roofs and reported an  
 220 NO<sub>2</sub> uptake of 300 μg/m<sup>2</sup>/h.

221 **Table.1.** Near steady-state NO<sub>2</sub> deposition velocities and plant uptake coefficients

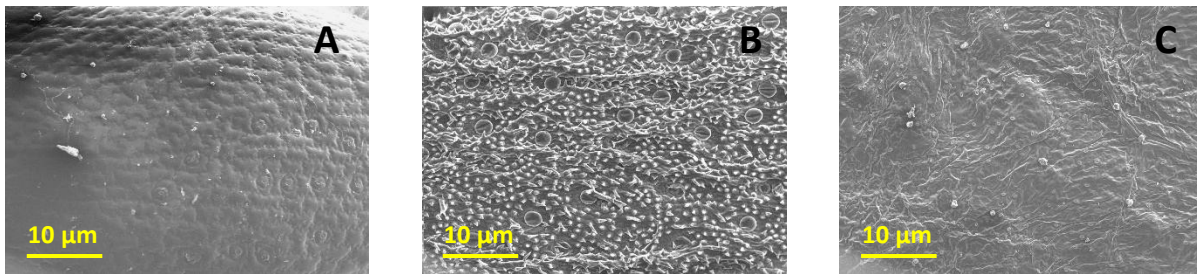
Plant	$v_{d(p)}^t$ (m/h)	$U_p^t$ ( $\mu\text{g}/\text{m}^2/\text{h}$ )
Sedum	2.99	282
Thyme	5.56	523
Heuchera	1.70	160

222 To better understand the uptake mechanisms and the difference between studied species, several  
223 experimental factors such as the stomata, water and chemical reactions were investigated.

224

225 - **Effect of stomata**

226 Leaf stomates are very important organs on the leaf surface as they control exchange of plants with  
227 the environment. In general, green plants affect air pollutants by taking up gaseous pollutants primarily  
228 through leaf stomates. The higher the density, the more CO<sub>2</sub> and gaseous pollutants can be absorbed or  
229 released [30].



230 **Fig.4.** SEM Images of the three studied plants: sedum (A), thyme (B), and heuchera (C).

231 Using SEM, we observed the stomates on each leaf and estimated the stomatal density and average  
232 stomatal areas by taking into consideration abaxial and adaxial sides. Highest stomata density was seen  
233 with heuchera followed by thyme and sedum ( $40 \text{ mm}^{-2} \pm 2$ ,  $6 \text{ mm}^{-2} \pm 2$ , and  $4 \text{ mm}^{-2} \pm 2$  respectively).  
234 However, thyme exhibited the largest stomatal area ( $8400 \pm 150 \mu\text{m}^2$ ) while those of sedum and heuchera  
235 were equal to  $5700 \pm 150 \mu\text{m}^2$  and  $1400 \pm 150$  respectively. This finding suggests that the higher stomatal  
236 area for thyme could be responsible for its better performance in removing NO<sub>2</sub>.

237 - **Effect of transpiration (surface reaction)**

238 A fraction of the consumption of NO<sub>2</sub> could be due to reactions with VOCs emitted by the plants. In  
239 general, NO<sub>2</sub> has a low reactivity towards VOCs. However, NO<sub>x</sub> might generate O<sub>3</sub> by photolysis under  
240 UV. As UV was not present, this pathway should be negligible. An alternative possibility is the decay of  
241 NO<sub>2</sub> through reaction with water leading to the formation of nitrous acid or HONO (process 1).

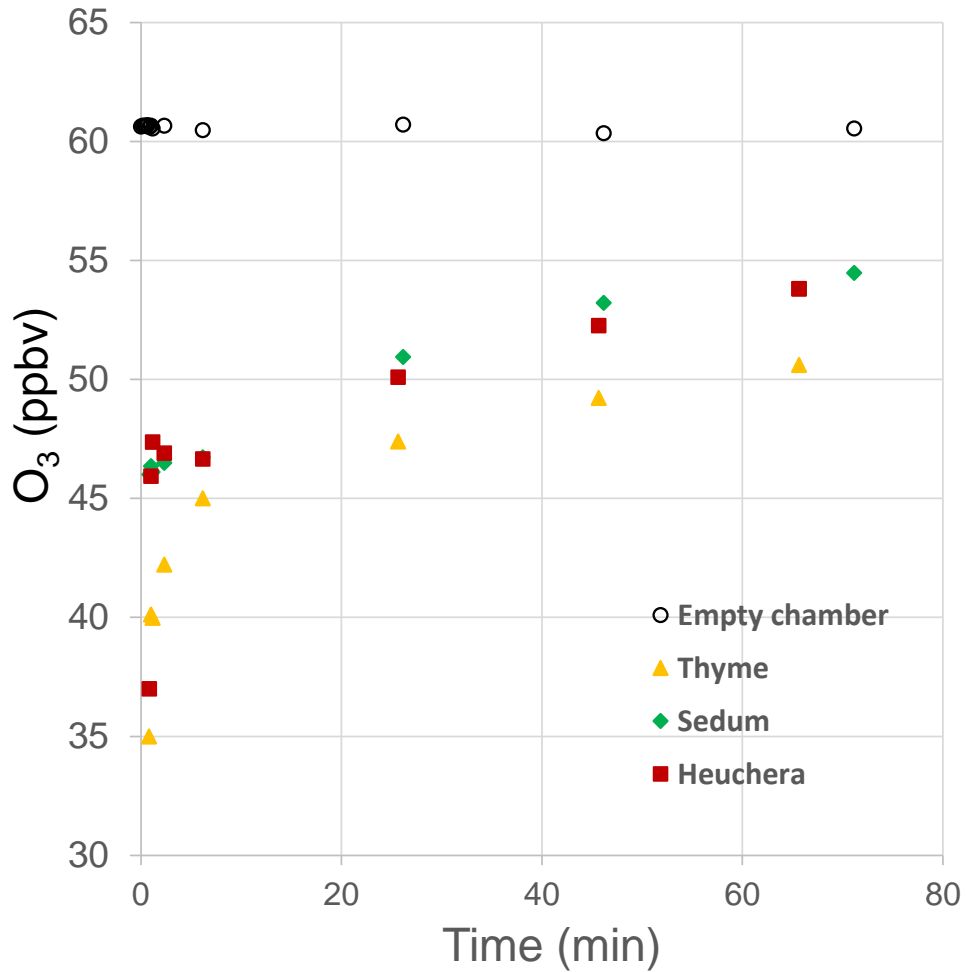


243 Such reaction is possible in the case of sedum particularly as it is an evergreen plant with moist leaves  
244 and transpiration can occur. In our experiments, sedum might release moisture after being irradiated and  
245 its water might react with NO<sub>2</sub> to yield HONO. We checked this hypothesis by performing experiments  
246 aiming to monitor the formation of HONO. This was done by including Na<sub>2</sub>CO<sub>3</sub> trap to sample HONO as  
247 described in the experimental section. In the same conditions as before, 1 g of leaves was irradiated under  
248 visible light for 1 h and the NO<sub>2</sub> uptake was monitored using sodium carbonate as a trap. The difference in  
249 the NO<sub>2</sub> uptake in the presence and absence of the trap reveals the uptake due to the reaction between NO<sub>2</sub>  
250 and water. Comparing the NO<sub>2</sub> values with and without the trap, we conclude that 55% of the uptake  
251 capacity was due to the reaction as shown in **process 1**. In the case of other species, no significant HONO  
252 production was observed, confirming that NO<sub>2</sub> uptake in the case of sedum is enhanced by surface water  
253 and its reaction with NO<sub>2</sub>. This finding highlights the importance of chemical reaction in addition to  
254 stomatal uptake in the overall performance of plant species and could have implication on the  
255 photochemistry of air pollutants since HONO can undergo direct photolysis to produce hydroxyl radicals  
256 (OH<sup>•</sup>).

257 3.1.2. O<sub>3</sub> uptake

258 **Fig.5.** illustrates the time evolution of the outlet concentration of O<sub>3</sub> in the case of an empty chamber  
259 and in presence of the three studied plants. The same steps were followed as the ones in part 2.1 using

260 same plants, irradiation system, and duration (1 hour of pre-conditioning in the chamber). As for the  
 261 experiment with NO<sub>2</sub>, thyme showed the highest O<sub>3</sub> uptake with a reduction of about 10 ppbv followed by  
 262 sedum and heuchera with a reduction of about 6-7 ppbv. **Table.2** shows the near steady-state O<sub>3</sub>  
 263 deposition velocities and plant uptake coefficients for the three studied plants calculated by averaging the  
 264 last 20 min of the exposure.



265 **Fig.5.** Empty chamber and outlet O<sub>3</sub> concentration for sedum, thyme, and heuchera.

266

267 **Table.2.** Near steady-state O<sub>3</sub> deposition velocities and plant uptake coefficients.

Plant	$v_{d(p)}^t$ (m/h)	$U_p^t$ (μg/m <sup>2</sup> /h)



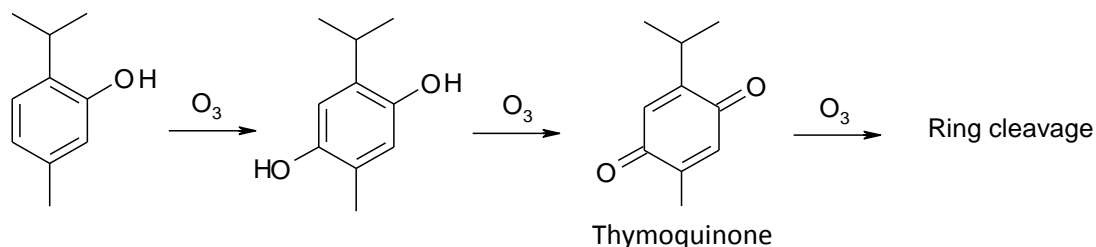
<b>Sedum</b>	2.69	317
<b>Thyme</b>	4.82	569
<b>Heuchera</b>	1.60	189
<b>Yang et.al [10]</b>	1.8	100-6500
<b>Curie et. Bass [11]</b>	0.18	-

268 The calculated values in our study are in agreement with those reported by Yang et al. [16] whereas  
269 the study of Curie et Bass [20] showed lower values compared to those found here.

270 - **Effect of thyme volatile metabolites**

271 While the higher stomatal area can be responsible for the better performance of thyme in removing O<sub>3</sub>,  
272 O<sub>3</sub> can potentially react with plant volatile metabolites particularly in the case of thyme which is known to  
273 release several terpenes in addition to thymol. For these reasons, thyme was selected as the main species  
274 to study in the following experiments. For a simpler approach, experiments were undertaken with one of  
275 the major emitted VOC, thymol (a phenolic derivative), first in solution to examine the feasibility of  
276 thymol degradation by O<sub>3</sub> and to facilitate the identification of by-products. O<sub>3</sub> reactions in solutions can  
277 be easier to perform and could provide a first indication of possible heterogeneous reactions between  
278 thymol and O<sub>3</sub> on leaves. Water can also be present on leaf surface and could participate in the reaction  
279 mechanisms. Following this feasibility test, additional experiments on thyme leaves were carried out to  
280 mimic realistic conditions and to investigate the heterogeneous reactivity of thyme volatiles with O<sub>3</sub>.

281 *Reaction of thymol with ozone in solution.* We prepared a 20 ml solution of thymol (2x10<sup>-4</sup> M) in ACN  
282 and O<sub>3</sub> at a concentration of 4 ppm was bubbled into it for almost 6 h. Results were monitored by HPLC-  
283 DAD analysis that showed that 50 % of thymol was degraded. The percentage of degradation is related to  
284 ozone and thymol concentrations. According to a study on the catalytic ozonation of thymol, the  
285 simplified proposed degradation mechanism is the following: the *para* and *ortho* positions of the  
286 hydroxyl on thymol are attacked by O<sub>3</sub> and hydroxyl radical. This leads to diols with a backbone of  
287 cymene (**Fig.6**). Several reactions then can take place prompting mineralization [25].



288 **Fig.6.** Thymol degradation pathway via the reaction with O<sub>3</sub>.

289 The GC-MS analysis of an experiment conducted on thymol and O<sub>3</sub> revealed the production of  
 290 Thymoquinone which corroborates the proposed mechanism.

291 *Reaction of thyme VOCs with ozone.* Two samples of detached thyme leaves (2 g) were introduced into  
 292 Pyrex flow-reactors, under irradiation with visible light. To monitor the effect of O<sub>3</sub>, the first sample (S1)  
 293 was not exposed to O<sub>3</sub> while the second (S2) was exposed to O<sub>3</sub> (153 ppbv). In both cases, the production  
 294 of VOC was monitored via sampling on sorbent tubes followed by ATD-GC-MS analysis.

295 **Table.3.** shows the four major terpenes emitted in addition to thymol. After 1 h of ozonation, their  
 296 levels decreased drastically as expected since terpenes are known to undergo oxidation by O<sub>3</sub>. This was  
 297 associated with the identification of various oxidation products such as linalool-oxide, keto-  
 298 limononaldehyde and thymoquinone. This finding confirms the role that plays thyme VOC metabolites in  
 299 the observed good performance for the removal of O<sub>3</sub>. However, while the uptake of ozone can be  
 300 enhanced by the emission of terpenes, one should consider the consequences of O<sub>3</sub> reactions with terpenes  
 301 since it can lead to the formation of secondary organic aerosols (SOA) [31]. Unfortunately, this was not  
 302 confirmed here but future experiments are needed to measure the possible emission of ultrafine particles  
 303 due to reaction of O<sub>3</sub> with thyme volatiles, and to estimate its impact on air pollution.

304

305 **Table.3.** Major VOC products identified in S1 and S2.

Sample	VOC collected mass (ng)				
	<i>Cymene</i>	<i>Limonene</i>	<i>Thymol</i>	<i>Eucalyptol</i>	<i>Linalool</i>
<b>S1 (no O<sub>3</sub>)</b>	12.6	8.5	22.5	13.2	31.3
<b>S2 (with O<sub>3</sub>)</b>	0.4	Non detected	Non detected	0.3	1.6

306 3.2. Depollution capacity of thyme full-size plant

307 3.2.1. NO<sub>2</sub>/O<sub>3</sub> uptakes

308 These following experiments were conducted using a small thyme plant (with an estimated total leaf  
309 area of 500 cm<sup>2</sup>) which was pre-conditioned in the big reactor (12 L) with 1 h visible light irradiation  
310 while soil was fully covered during experiments to ensure the least interference possible. After 1h of  
311 exposure to NO<sub>2</sub> (50 ppbv) the NO<sub>2</sub> concentration dropped to reach a near-steady state around 10 ppbv.  
312 Using eq.(1) and (2) we calculated a  $v_{d(p)}^t$  of 3.84 m/h. In the case of O<sub>3</sub>, same conditions were used as  
313 with detached leaves with the exception of O<sub>3</sub> inlet concentration which was increased to 110 ± 3 ppbv to  
314 reduce measurement uncertainty. Under these conditions, O<sub>3</sub> concentration dropped by around 91 ppbv to  
315 reach 19 ppbv after 1h of exposure (Fig. SI-4). Assuming a near steady-state condition we obtained a  
316  $v_{d(p)}^t$  of 4.65 m/h. These values are comparable with those obtained using detached leaves particularly  
317 when considering the uncertainty in the estimation of total leaf area, presence of soil, emission of volatile  
318 metabolites and the measurement uncertainty. It is noteworthy that a small production of NO was  
319 observed when thyme plant was irradiated which was not detected with detached leaves. NO is a key  
320 signaling molecule in plant physiology. However, its production in photosynthetic organisms remains  
321 partially unresolved. The best characterized NO production route involves the reduction of nitrite (NO<sub>2</sub><sup>-</sup>)  
322 to NO via different non-enzymatic or enzymatic mechanisms. To better characterize the role of soil in the  
323 production of NO and the uptake of pollutants, additional experiments using soil only were carried out.

324 - **Effect of soil on NO<sub>x</sub> production and uptake and of O<sub>3</sub> uptake**

325 Soil, as well, is used on green roofs so its uptake towards  $\text{NO}_2$  and  $\text{O}_3$  in addition to its  $\text{NO}_x$   
326 production were studied. In these experiments the same soil used for thyme was studied here.

327 *NO<sub>x</sub> production.* After 1 h of visible light irradiation, a mixture of  $\text{N}_2$  and  $\text{O}_2$  (pure synthetic air) was  
328 passed through the reactor containing the soil to monitor the  $\text{NO}/\text{NO}_2$  production. Studied soil was either  
329 wet or dry, but the steps were the same in both cases. Only  $\text{NO}$  was produced at a level of  $\approx 20$  ppbv in the  
330 case of dry soil, and  $\approx 10$  ppbv in that of wet soil (**Fig.SI-5**). Irrigation, N-fertilizers, and bacteria are  
331 known to be responsible for  $\text{NO}_2$  production [32]. In our experiments, the adsorbed  $\text{NO}_2$  is probably  
332 undergoing reactions producing  $\text{NO}_{(g)}$  in case of both dry and wet soils; or reacting with water producing  
333 ions e.g.  $\text{NO}_2^-$  and  $\text{NO}_3^-$  (case of wet soil).

334 *NO<sub>2</sub>/O<sub>3</sub> uptake.* The same experimental steps were followed as in section 3.2. In the case of  $\text{O}_3$   
335 (see Fig. SI-4), the reduction in concentration ( $\Delta$ ) for exposed soil ranged between 85 (dry) and 88 (wet)  
336 ppbv which is very close to that observed with thyme (91 ppbv). This suggests that soil can also be as  
337 effective in removing  $\text{O}_3$  and could contribute to increase the overall performance of green roofs. On the  
338 other hand, soil contributed to the removal of 15 ppbv (wet) to 35 ppbv (dry) of  $\text{NO}_2$  as compared with  
339 about 40 ppbv for thyme (Fig. SI-6) indicating that the thyme plant is more effective in removing  $\text{NO}_2$ .  
340 The higher  $\text{NO}_2$  uptake by dry soil is likely associated with the higher surface area available for adsorption  
341 as compared with wet soil which can be partially saturated with water.

#### 342 4. CONCLUSION

343 Natural air pollution mitigation approaches are needed to help improve air quality especially in  
344 urbanized areas. One promising recommended approach is the use of green roofs. In this study, we  
345 developed a new  $\text{NO}_2/\text{O}_3$  bench-scale experimental system to measure the depollution performance of  
346 different green roofs species.

347 After the screening of several species, 3 species were found to be the most efficient for the  
348  $\text{NO}_2/\text{O}_3$  uptakes: *sedum sexangulare*, *thymus vulgaris*, and *heuchera americana L.* They offer a diversity

349 between being aesthetically pleasant, drought tolerant, climate resilient, and exhibiting good uptakes. NO<sub>2</sub>  
350 uptake coefficients ranged from 160 to 523 μg/m<sup>2</sup>/h while that of O<sub>3</sub> varied between 189 and 569 μg/m<sup>2</sup>/h.  
351 These findings are in accordance with previously reported data using the big-leaf dry deposition models.  
352 Nevertheless, values were relatively higher in our experiments possibly due to other mechanisms than dry  
353 deposition (adsorption) such as the reactions between the VOCs and O<sub>3</sub> especially in the case of thyme,  
354 and between NO<sub>2</sub> and water in the case of the evergreen plant: sedum -which are not considered yet in  
355 models. If we apply our experimental results using the existing model [16] by taking the average  
356 deposition velocity in our experiments (0.095 m/h for NO<sub>2</sub> and 0.084 m/h for O<sub>3</sub>), the total uptake by the 3  
357 species (sedum, thyme, and heuchera) could reach 9 kg/ha/year of NO<sub>2</sub> and around 13.6 kg/ha/year of O<sub>3</sub>.  
358 Assuming that Paris has around 76 ha of green roofs and walls (2016) [33], and if the three species  
359 investigated in this study were to be used, one can estimate that 683 kg/year of NO<sub>2</sub> and 1037 kg/year of  
360 O<sub>3</sub> can be mitigated.

361 While our study focused only on the uptake of two air pollutants, additional research should be  
362 carried to measure the performance of green roof species towards PM<sub>2.5</sub> and to investigate the potential  
363 formation of SOA. In addition, our experimental design does not consider some important variables such  
364 as the effects of humidity, lighting spectrum/intensity changes, nor the diurnal and seasonal cycles of the  
365 plant. In addition, field evaluation of laboratory results should be carried in order to better understand the  
366 effects of seasonality and weather conditions on the depollution performance of green roofs.

## 367 **5. ASSOCIATED CONTENT**

### 368 **Supporting information (e-component) 6 figures**

369 The Volatile Organic Compounds emitted by thyme obtained by headspace-GC-MS. The small  
370 and big reactors containing the detached leaves and the full-size plant/soil. The light spectrum of the  
371 lamps used in our experiments for irradiation. O<sub>3</sub> uptakes by Thyme and soil (wet and dry) after

372 irradiation. NO production by the soil (wet and dry) after being irradiated by visible light for 1 h. NO<sub>2</sub>  
373 uptakes by the soil (wet and dry) after 1 h of visible light irradiation.

#### 374 **ACKNOWLEDGEMENTS**

375 Y. ARBID thanks Peng CHENG for his technical assistance, Adelina DAVID and Mr. Yann  
376 FASCHINETTI for the microscopy analysis, and Mr. Martin LEREMBOURE regarding the LC-MS  
377 analysis.

#### 378 **FUNDING SOURCES**

379 This work was supported by the University of Clermont Auvergne and the French Ministry of  
380 Higher Education and Research.

#### 381 **REFERENCES**

- 382 [1] World Health Organization, Air pollution, (2019). <https://www.who.int/health-topics/air-pollution>.
- 383 [2] J. Zhao, X. Xi, Q. Na, S. Wang, S.N. Kadry, P.M. Kumar, The technological innovation of hybrid  
384 and plug-in electric vehicles for environment carbon pollution control, *Environ. Impact Assess.*  
385 *Rev.* 86 (2021). <https://doi.org/10.1016/j.eiar.2020.106506>.
- 386 [3] R. Zalakeviciute, Y. Rybarczyk, J. López-Villada, M.V. Diaz Suarez, Quantifying decade-long  
387 effects of fuel and traffic regulations on urban ambient PM<sub>2.5</sub> pollution in a mid-size South  
388 American city, *Atmos. Pollut. Res.* 9 (2018) 66–75. <https://doi.org/10.1016/j.apr.2017.07.001>.
- 389 [4] M. Granovskii, I. Dincer, M.A. Rosen, Air pollution reduction via use of green energy sources for  
390 electricity and hydrogen production, *Atmos. Environ.* 41 (2007) 1777–1783.  
391 <https://doi.org/10.1016/j.atmosenv.2006.10.023>.
- 392 [5] X. Tang, O. Rosseler, S. Chen, S. Houzé de l’Aulnoit, M.J. Lussier, J. Zhang, G. Ban-Weiss, H.  
393 Gilbert, R. Levinson, H. Destailats, Self-cleaning and de-pollution efficacies of photocatalytic  
394 architectural membranes, *Appl. Catal. B Environ.* 281 (2021) 119260.  
395 <https://doi.org/10.1016/j.apcatb.2020.119260>.
- 396 [6] X. Tang, L. Ughetta, S.K. Shannon, S. Houzé de l’Aulnoit, S. Chen, R.A.T. Gould, M.L. Russell,  
397 J. Zhang, G. Ban-Weiss, R.L.A. Everman, F.W. Klink, R. Levinson, H. Destailats, De-pollution  
398 efficacy of photocatalytic roofing granules, *Build. Environ.* 160 (2019) 106058.  
399 <https://doi.org/https://doi.org/10.1016/j.buildenv.2019.03.056>.
- 400 [7] J. Chen, C. Poon, Photocatalytic construction and building materials: From fundamentals to  
401 applications, *Build. Environ.* 44 (2009) 1899–1906.

- 402 <https://doi.org/https://doi.org/10.1016/j.buildenv.2009.01.002>.
- 403 [8] M. Krichevskaya, S. Preis, A. Moiseev, N. Pronina, J. Deubener, Gas-phase photocatalytic  
404 oxidation of refractory VOCs mixtures: Through the net of process limitations, *Catal. Today*. 280  
405 (2017) 93–98. <https://doi.org/10.1016/j.cattod.2016.03.041>.
- 406 [9] A. Palla, I. Gnecco, L.G. Lanza, Unsaturated 2D modelling of subsurface water flow in the coarse-  
407 grained porous matrix of a green roof, *J. Hydrol.* 379 (2009) 193–204.  
408 <https://doi.org/10.1016/j.jhydrol.2009.10.008>.
- 409 [10] H. Liu, F. Kong, H. Yin, A. Middel, X. Zheng, J. Huang, H. Xu, D. Wang, Z. Wen, Impacts of  
410 green roofs on water, temperature, and air quality: A bibliometric review, *Build. Environ.* 196  
411 (2021) 107794. <https://doi.org/10.1016/j.buildenv.2021.107794>.
- 412 [11] J. Mentens, D. Raes, M. Hermy, Green roofs as a tool for solving the rainwater runoff problem in  
413 the urbanized 21st century?, *Landsc. Urban Plan.* 77 (2006) 217–226.  
414 <https://doi.org/10.1016/j.landurbplan.2005.02.010>.
- 415 [12] L.M. Cook, T.A. Larsen, Towards a performance-based approach for multifunctional green roofs:  
416 An interdisciplinary review, *Build. Environ.* 188 (2021) 107489.  
417 <https://doi.org/10.1016/j.buildenv.2020.107489>.
- 418 [13] Y. He, H. Yu, A. Ozaki, N. Dong, S. Zheng, Long-term thermal performance evaluation of green  
419 roof system based on two new indexes: A case study in Shanghai area, *Build. Environ.* 120 (2017)  
420 13–28. <https://doi.org/10.1016/j.buildenv.2017.04.001>.
- 421 [14] T. Van Renterghem, D. Botteldooren, Numerical evaluation of sound propagating over green roofs,  
422 *J. Sound Vib.* 317 (2008) 781–799. <https://doi.org/10.1016/j.jsv.2008.03.025>.
- 423 [15] D.B. Rowe, Green roofs as a means of pollution abatement, *Environ. Pollut.* 159 (2011) 2100–  
424 2110. <https://doi.org/10.1016/j.envpol.2010.10.029>.
- 425 [16] J. Yang, Q. Yu, P. Gong, Quantifying air pollution removal by green roofs in Chicago, *Atmos.*  
426 *Environ.* 42 (2008) 7266–7273. <https://doi.org/10.1016/j.atmosenv.2008.07.003>.
- 427 [17] D.J. Nowak, D.E. Crane, J.C. Stevens, Air pollution removal by urban trees and shrubs in the  
428 United States, *Urban For. Urban Green.* 4 (2006) 115–123.  
429 <https://doi.org/10.1016/j.ufug.2006.01.007>.
- 430 [18] V. Etyemezian, S. Ahonen, D. Nikolic, J. Gillies, H. Kuhns, D. Gillette, J. Veranth, Deposition and  
431 removal of fugitive dust in the arid southwestern united states: Measurements and model results, *J.*  
432 *Air Waste Manag. Assoc.* 54 (2004) 1099–1111.  
433 <https://doi.org/10.1080/10473289.2004.10470977>.
- 434 [19] N.W. Lepp, Planting Green Roofs and Living Walls, *J. Environ. Qual.* 37 (2008) 2408–2408.  
435 <https://doi.org/10.2134/jeq2008.0016br>.
- 436 [20] B.A. Currie, B. Bass, Estimates of air pollution mitigation with green plants and green roofs using  
437 the UFORE model, *Urban Ecosyst.* 11 (2008) 409–422. [https://doi.org/10.1007/s11252-008-0054-](https://doi.org/10.1007/s11252-008-0054-y)  
438 [y](https://doi.org/10.1007/s11252-008-0054-y).
- 439 [21] A.F. Speak, J.J. Rothwell, S.J. Lindley, C.L. Smith, Urban particulate pollution reduction by four

- 440 species of green roof vegetation in a UK city, *Atmos. Environ.* 61 (2012) 283–293.  
441 <https://doi.org/10.1016/j.atmosenv.2012.07.043>.
- 442 [22] O.A. Abbass, D.J. Sailor, E.T. Gall, Ozone removal efficiency and surface analysis of green and  
443 white roof HVAC filters, *Build. Environ.* 136 (2018) 118–127.  
444 <https://doi.org/10.1016/j.buildenv.2018.03.042>.
- 445 [23] P. Ramasubramanian, I. Luhung, S.B.Y. Lim, S.C. Schuster, O. Starry, E.T. Gall, Impact of green  
446 and white roofs on air handler filters and indoor ventilation air, *Build. Environ.* 197 (2021)  
447 107860. <https://doi.org/https://doi.org/10.1016/j.buildenv.2021.107860>.
- 448 [24] G. Pérez, C. Chocarro, A. Juárez, J. Coma, Evaluation of the development of five *Sedum* species  
449 on extensive green roofs in a continental Mediterranean climate, *Urban For. Urban Green.* 48  
450 (2020) 126566. <https://doi.org/10.1016/j.ufug.2019.126566>.
- 451 [25] L. Wang, A. Liu, Z. Zhang, B. Zhao, Y. Xia, Y. Tan, Catalytic ozonation of thymol in reverse  
452 osmosis concentrate with core/shell Fe<sub>3</sub>O<sub>4</sub>@SiO<sub>2</sub>@Yb<sub>2</sub>O<sub>3</sub> catalyst: Parameter optimization and  
453 degradation pathway, *Chinese J. Chem. Eng.* 25 (2017) 665–670.  
454 <https://doi.org/10.1016/j.cjche.2016.10.017>.
- 455 [26] U. Weerakkody, J.W. Dover, P. Mitchell, K. Reiling, Quantification of the traffic-generated  
456 particulate matter capture by plant species in a living wall and evaluation of the important leaf  
457 characteristics, *Sci. Total Environ.* 635 (2018) 1012–1024.  
458 <https://doi.org/10.1016/j.scitotenv.2018.04.106>.
- 459 [27] D. Palma, Y. Arbid, M. Sleiman, P. De Sainte-Claire, C. Richard, New Route to Toxic Nitro and  
460 Nitroso Products upon Irradiation of Micropollutant Mixtures Containing Imidacloprid: Role of  
461 NO<sub>x</sub> and Effect of Natural Organic Matter, *Environ. Sci. Technol.* 54 (2020) 3325–3333.  
462 <https://doi.org/10.1021/acs.est.9b07304>.
- 463 [28] D. Poppendieck, H. Hubbard, M. Ward, C. Weschler, R.L. Corsi, Ozone reactions with indoor  
464 materials during building disinfection, *Atmos. Environ.* 41 (2007) 3166–3176.  
465 <https://doi.org/10.1016/j.atmosenv.2006.06.060>.
- 466 [29] O.A. Abbass, D.J. Sailor, E.T. Gall, Effectiveness of indoor plants for passive removal of indoor  
467 ozone, *Build. Environ.* 119 (2017) 62–70. <https://doi.org/10.1016/j.buildenv.2017.04.007>.
- 468 [30] B. Grant, I. Vatnick, Environmental correlates of leaf stomata density, *Teaching Issues and  
469 Experiments in Ecology*, TIEE Volume 1 (2004) 1–6. Ecological Society of America.  
470 ([www.tiee.ecoed.net](http://www.tiee.ecoed.net)).
- 471 [31] X. Chen, P.K. Hopke, W.P.L. Carter, Secondary Organic Aerosol from Ozonolysis of Biogenic  
472 Volatile Organic Compounds: Chamber Studies of Particle and Reactive Oxygen Species  
473 Formation, *Environ. Sci. Technol.* 45 (2011) 276–282. <https://doi.org/10.1021/es102166c>.
- 474 [32] C.H. Jaeger, R.K. Monson, M.C. Fisk, S.K. Schmidt, Seasonal partitioning of nitrogen by plants  
475 and soil microorganisms in an alpine ecosystem, *Ecology.* 80 (1999) 1883–1891.  
476 [https://doi.org/10.1890/0012-9658\(1999\)080\[1883:SPONBP\]2.0.CO;2](https://doi.org/10.1890/0012-9658(1999)080[1883:SPONBP]2.0.CO;2).
- 477 [33] M.A. Kleiber. A Paris, quel est l'impact réel de la végétalisation des toits.  
478 [https://www.lejdd.fr/JDD-Paris/a-paris-quel-est-limpact-reel-de-la-vegetalisation-des-toits-](https://www.lejdd.fr/JDD-Paris/a-paris-quel-est-limpact-reel-de-la-vegetalisation-des-toits-3798761)  
479 [3798761](https://www.lejdd.fr/JDD-Paris/a-paris-quel-est-limpact-reel-de-la-vegetalisation-des-toits-3798761).